

Chandra View of Pulsar Wind Nebula Tori

Aya Bamba^{1,2}, Koji Mori³, Shinpei Shibata⁴

ABSTRACT

The results from a systematic study of eleven pulsar wind nebulae with a torus structure observed with the *Chandra* X-ray observatory are presented. A significant observational correlation is found between the radius of the tori, r , and the spin-down luminosity of the pulsars, \dot{E} . A logarithmic linear fit between the two parameters yields $\log r = (0.57 \pm 0.22) \log \dot{E} - 22.3 \pm 8.0$ with a correlation coefficient of 0.82, where the units of r and \dot{E} are pc and ergs s⁻¹, respectively. The value obtained for the \dot{E} dependency of r is consistent with a square root law, which is theoretically expected. This is the first observational evidence of this dependency, and provides a useful tool to estimate the spin-down energies of pulsars without direct detections of pulsation. Applications of this dependency to some other samples are also shown.

Subject headings: pulsars: general — stars: neutron — shock waves — X-rays: stars

1. Introduction

Active pulsars eject relativistic pulsar winds comprised of relativistic particles and magnetic field. Such winds are terminated by a strong shock where pressure balance is attained with the ambient medium. High energy particles diffusing out in the downstream of the shock emit radio to very high energy gamma-rays via synchrotron or inverse Compton processes, which are observed as pulsar wind nebulae (PWNe). The distance from the pulsar to the termination shock, r_s , is expected to be

$$r_s = \left(\frac{\dot{E}}{4\pi c \eta P_{\text{ext}}} \right)^{1/2}, \quad (1)$$

where \dot{E} , c , η , P_{ext} are the spin-down luminosity of the pulsar, the light speed, the filling factor, and the external pressure (Rees & Gunn 1974). The

size of shocks should be roughly 0.01–0.1 pc with typical parameters of PWNe (Kennel & Coroniti 1984). In the case of a weakly-magnetized pulsar wind, which is believed to apply to most of these systems, particle energy density dominates that of magnetic field energy at the shock in which the emissivity of synchrotron radiation is relatively low. Then, the shock is generally invisible with the current instruments except for the brightest example, the Crab Nebula (Weisskopf et al. 2000). The equipartition between particle and magnetic field energy, at which the Synchrotron emissivity is the highest, is reached at a distance of a few times of r_s , as the post shock flow decelerates (Kennel & Coroniti 1984). Considering that most of the pulsar wind energy is blown near the equatorial plane and that Synchrotron cooling becomes efficient at the outer region, a torus-like structure is expected in this system whose radius is a few times of r_s .

The *Chandra* X-ray observatory has actually revealed the torus (and jet-like) structures from several PWNe thanks to the excellent spatial resolution of 0.5 arcsec (c.f., Kargaltsev & Pavlov 2008). Ng & Romani (2004) developed a sophisticated method to fit three-dimensional model to the tori, which they applied to the *Chandra* data of several PWNe (Ng & Romani 2008a), providing most reliable values of the torus radius. Since the

¹ School of Cosmic Physics, Dublin Institute for Advanced Studies 31 Fitzwilliam Place, Dublin 2, Ireland abamba@cp.dias.ie

² ISAS/JAXA Department of High Energy Astrophysics 3-1-1 Yoshinodai, Sagami-hara, Kanagawa 229-8510, JAPAN

³ Department of Applied Physics, Faculty of Engineering University of Miyazaki, 1-1 Gakuen Kibana-dai Nishi, Miyazaki, 889-2192, Japan

⁴ Department of Physics, Yamagata University 1-4-12 Kojirakawa, Yamagata 990-8560, Japan

termination shock radius is expected to be proportional to the square root of the spin-down luminosity, the torus radii may scale in the same way as the shock radii, if so, one would expect a correlation between the torus radii and the spin-down luminosities following the square-root law. In this paper, we confirm this relationship for the first time, and show its astrophysical use for some PWNe.

2. Samples

In this paper, we used 11 samples for our study with the following criteria. *Chandra* observed several tens of PWNe (Kargaltsev & Pavlov 2008). Thanks to the excellent spatial resolution of the X-ray telescope, equatorial tori and polar jet structures are discovered in more than 10 PWN systems. Ng & Romani (2004, 2008a) measured the torus radius of 10 PWNe with the developed method by Ng & Romani (2004). Romani et al. (2005) uses the same method to B1706–44, and we added this PWN to our sample.

Table 1 shows details of our samples. Our samples are so young that the pulsar wind is still strong and morphological distortion due to pulsar motion is relatively small yet; old systems sometimes show cometary structure controlled by this effect. Actually, they are categorized to “PWNe with toroidal components” in Kargaltsev & Pavlov (2008) except for J0537–6910, which has a cometary nebula (Chen et al. 2006). Ng & Romani (2008a) derived the size of its torus (r_{arcsec} in Table 1) after subtracting the diffuse nebula, and we use the parameters by Ng & Romani (2008a). The latest distance estimates are used to calculate the physical radius of the tori (r in Table 1) with references in Table 1.

3. Results

In this section, we search for a correlation between the torus radius r and spin-down luminosity \dot{E} . Figure 1 represents the plot of r as a function of \dot{E} . Uncertainties of r in the figure are obtained simply by multiplication of the nebula distances and the statistical uncertainties in apparent torus radii determined by Ng & Romani (2004, 2008a) and Romani et al. (2005). It is apparent that there is a strong positive correlation between $\log \dot{E}$ and $\log r$, yielding a correlation coefficient

of 0.82. This power-law like correlation is as expected as we review in § 1. On the other hand, it is also obvious that there is a non-negligible fluctuation beyond a simple power-law function owing to the statistical uncertainties. These facts suggest that r is certainly a function of \dot{E} but that there are other hidden parameters which give a larger fluctuation to this relation than the given statistical uncertainties. We will discuss possible origin of the parameters later. We thus fit the data weighting them equally with a power-law function,

$$\log r = \alpha \log \dot{E} + \beta \quad , \quad (2)$$

where α and β are constant values. We obtained

$$\begin{aligned} \alpha &= 0.57 \pm 0.22 \quad , \\ \beta &= -22.3 \pm 8.0 \quad , \end{aligned} \quad (3)$$

respectively. The best-fit model is shown in Figure 1 with a thick solid line.

In order to check our result from a different point view, we calculated the correlation coefficient between $\log \dot{E}$ and r/\dot{E}^α , which should be 0 with the best-fit α . Figure 2 shows the relation between α and the correlation coefficient. We can see that the correlation coefficient becomes close to 0 when α is between 0.5 and 0.6. This result indicates again that α is around 0.5–0.6.

The value of α agrees well with the expected 0.5 (eq.(1)). It also implies that the torus radius scales in the same manner as the radius of the termination shock. If we fix α to be 0.5, the equation becomes

$$\log r = 0.5 \log \dot{E} - 19.6 \pm 0.2 \quad . \quad (4)$$

This result is also shown in Figure 1 with a thick dashed line.

There are three samples which are well below the best-fit lines: Vela, PSR J2229+6114, and PSR J1124–5916. The former two are known to show clear evidences of interaction with ejecta or interstellar medium (LaMassa et al. 2008; Kothes et al. 2001). In such a case, as is indicated by Eq.(1), the torus radii could be smaller confined by higher external pressure compared to those without interaction with surrounding medium. As for the last one, Park et al. (2004) showed that the reverse shock has not yet begun to interact with it. However, the latest 510 ksec

Chandra observation revealed the almost 3 times larger torus compared with that seen in the previous 50 ksec Chandra observation which Ng & Romani (2008a) analyzed (Park et al. 2007).

Taking these facts into account, we made another fit where Vela and PSR J2229+6114 are excluded and the original value of PSR J1124–5916 is multiplied by a factor of 3. In this fit, we found the better correlation factor of 0.93 and obtained the best-fit model of

$$\log r = (0.49 \pm 0.12) \log \dot{E} - 19.2 \pm 4.7 \quad (5)$$

as shown with a thin solid line in Figure 1.

We also searched for correlation between the torus radius and other physical parameters, such as age of PWNe, magnetic field, and so on, but could not find any significant correlation.

4. Discussion

4.1. Termination shocks and tori

Eq.(3) shows that the tori radii (r) show a square root dependance on \dot{E} like the termination shock radii (r_s): This is the first clue of the termination shocks in PWNe.

Here, we introduce $z \equiv r/r_s$, the ratio between the radii of observed torus and the shock. The value of z can be common among pulsars in spite of different pulsar parameters and environment. Assuming eq.(4),

$$\begin{aligned} z &= r/r_s \\ &= 10^\beta (4\pi c \eta P_{ext})^{1/2} \\ &= 1.9_{-0.7}^{+1.1} \left(\frac{\eta}{1}\right)^{1/2} \left(\frac{P_{ext}}{1.6 \times 10^{-9} [\text{g cm}^{-1} \text{s}^{-2}]}\right)^{1/2} \quad (6) \end{aligned}$$

When the temperature, number density, and filling factor of external environment of the termination shock is 1 keV, 1 cm^{-3} , and 1, ($P_{ext} = 1.6 \times 10^{-9} \text{ g cm}^{-1} \text{s}^{-2}$), the ratio of radii of X-ray torus and termination shock is almost unity. The X-ray emission should come from the outside region of the termination shock according to Kennel & Coroniti (1984), which supports our result.

The best-fit α , 0.57, is slightly larger than the theoretical value in eq.(1). The data scatter seems to be larger at lower values for spin-down energy.

It could be due to an age effect. The fitting without Vela and J2229+6114, which interact with ejecta or interstellar medium, shows larger radius and smaller dispersion. This result supports our scenario.

4.2. Fluctuation of thermal parameters

Figure 1 shows that the data points have rather large scatter to the best-fit line. We here discuss on the possible origin of the fluctuation. Since \dot{E} is derived solely from timing information which generally has much higher accuracy than other observable quantities, we concentrate on other parameters, such as thermal parameters like r , η and P_{ext} , and distance.

We first estimate how large fluctuation of r is required to reproduce the correlation coefficient of 0.82 by a simple simulation. A single trial of the simulation generates 11 samples from a parent population with fluctuated environment, which is simulated by log-normal variation in the product ηP_{ext} with a given standard deviation of σ_0 . We made 1000 trials with a given σ_0 to calculate an expected correlation coefficient $\langle A \rangle$ and the probability for A to be larger than 0.82. Table 2 lists the expected correlation coefficient and the probability with different σ_0 's. The simulation suggest that the observed scatter is explained if $\sigma_0 \sim 0.6$, i.e., if fluctuation in ηP_{ext} is a factor of ~ 4 .

One may think that the distance uncertainty may be a primary source of this fluctuation. If it is the case, we need a factor 2 fluctuation of distance since the fluctuation of the torus radii is linearly connected to the distance uncertainty, which is the square root of ηP_{ext} fluctuation. Although distance to astronomical bodies is not always constrained very well, the factor of 2 appears to be too large to be attributed to the distance uncertainty alone especially for such famous and well-studied samples. One of the most famous and general measurement method of distance to supernova remnants (SNRs) is to use the Σ — D relation (e.g., Case & Bhattacharya 1998); the distances to more than 200 SNRs are estimated using the surface brightness at 1 GHz and diameter relation, although there is $\sim 40\%$ dispersion between distance from their method and those from other methods. This is because Σ — D relations can be used to estimate properties of ensembles of SNRs, not for individual one, as Case & Bhattacharya (1998)

mentioned. Our relation on the PWN tori can be used in similar way to Σ – D relation to estimate their distance.

The fluctuations of η and P_{ext} result in that of r_s , and thus that of r as well. A fluctuation of r by a factor of 2 roughly corresponds to that of ηP_{ext} by a factor of 4. This level of fluctuation could easily occur about P_{ext} . The density of external gas, which is inside of SNR shells, differ by about three orders of magnitude from SNR to SNR, from ~ 0.1 (SN 1006; Yamaguchi et al. 2008) up to ~ 200 (Cas A; Lazendic et al. 2006). Thus, we believe that the variation of P_{ext} is the primary cause of the scatter. Actually, the torus of Vela X, which evidently interacts with ejecta, has smaller radius relative to the best fit function, which may be due to the larger P_{ext} effect among our samples. Samples without these PWNe shows clearly tighter correlation. The fluctuation of ηP_{ext} is also estimated with eq.(5) to be 2.5, as shown in Table 3, which is much smaller than those with all samples.

The interesting thing is that all of the samples with small torii are categorized into combined type SNRs, which have radio shell and PWNe. It could be due to that SNRs with bright shells have higher densities inside the remnants. The detailed systematic and observational study of P_{ext} for individual objects might give a better explanation of this fluctuation although it is beyond the scope of this paper.

All we mention above are the “negative” factors which tend to wash out the correlation between \dot{E} and r . Nonetheless, we find it with relatively high significance, which in turn suggests the robustness of this correlation.

5. Application

Once the correlation between \dot{E} and r is established, it will provide a useful tool to estimate the spin-down energy of pulsars without direct detections of pulsation, although the large error range prevent us from precise parameters determinations. We show some examples of the application. In this section, we cite eq.(3) although using eq.(5) does not alter the results here so much.

5.1. \dot{E} determination for G0.9+0.1

With eq.(3), we can estimate the spin-down luminosity of PWNe from the radius of tori, without information of pulsation.

Let us consider the example of G0.9+0.1. The SNR G0.9+0.1 has a X-ray bright PWN in the Galactic center region. Gaensler et al. (2001) resolved the PWN with Chandra. The size and flux are $5 \text{ arcsec} \times 8 \text{ arcsec}$ and $6.6 \times 10^{-12} \text{ ergs cm}^{-2} \text{ s}^{-1}$ in the 2–10 keV band, respectively. The torus radius should be about half of the longer extension, 4 arcsec, or 0.16 pc with the distance of 8.5 kpc. With this value and eq.(3), we can estimate the $\log \dot{E}$ of G0.9+0.1 to be 37.7. There is no difference whether we use eq.(4) or eq.(3).

Possenti et al. (2002) discovered the empirical relation between \dot{E} and the 2–10 keV luminosity L_X (ergs s^{-1}) of PWNe of

$$\log L_X = 1.34 \log \dot{E} - 15.34 \quad , \quad (7)$$

although the dispersion is large (c.f. Kargaltsev & Pavlov 2008). We can estimate the spin-down luminosity of G0.9+0.1 independently from their relation to be $\log \dot{E} = 37.4$, which shows very good agreement with our estimate.

Very recently, Camilo et al. (2009) discovered coherent pulsation from the central pulsar with the period and the period derivative of 52 ms and $1.5557 \times 10^{-13} \text{ s s}^{-1}$, respectively. The resultant spin-down energy is $\log \dot{E}$ of 37.6, which also shows good agreement with our result.

5.2. \dot{E} determination for G328.4+0.2

Gelfand et al. (2007) found an extended structure in the PWN G328.4+0.2 with *XMM-Newton* with the size of $\sim 1 \text{ arcsec}$, or 0.09 pc at 17 kpc (Gelfand et al. 2007). The coherent pulsation has not been detected yet. We can estimate the spin-down luminosity in the same way as for G0.9+0.1 to be $\log \dot{E} = 37.3$. This is totally consistent with previous estimation using Possenti et al. (2002), $\log \dot{E} = 37.2$ (Gelfand et al. 2007).

5.3. Distance determination of PSR J1846–0258

PSR J1846–0258 in SNR Kes 75 is one of the mysterious PWNe with soft-Gamma-ray repeater like flares (Gavriil et al. 2008; Kumar & Safi-Harb

2008). The spin-down luminosity is rather large, $\log \dot{E}$ of 36.91. However, the distance of this interesting source is still unclear: Becker & Helfand (1984) estimated that the distance is 19–21 kpc, whereas Leahy & Tian (2008) suggests that this system is much nearer, 5.1–7.5 kpc.

Eq.(3) and the spin-down luminosity indicate a torus radius of 0.07 pc, whereas the detected torus by Ng et al. (2008b) has the radius of 10 arcsec. It suggests that the expected distance from \dot{E} – r relation is about 1.1 kpc. It is too small compared with other distance estimates, or in other word, the torus radius is too large. This would indicate that either an exceptionally low ambient pressure or the pulsar provides additional pressure from the inside. It could be important information to understand the origin of magnetars, which is still hotly debated (e.g., Vink & Kuiper 2006; Ferrario & Wickramasinghe 2006; Duncan & Thompson 1992; Gavriil et al. 2008). Systematic study of PWN torii of magnetars should be done although we have few samples until now (Rea et al. 2009; Vink & Bamba 2009).

5.4. Torus search of DEM L241

The SNR DEM L241 in the Large Magellanic Cloud (LMC) has a compact X-ray source in its center detected with *XMM-Newton* (Bamba et al. 2006). The flux and photon index are 5.0×10^{-12} in the 2.0–10.0 keV band and 1.57, respectively. The spin-down luminosity expected by Possenti et al. (2002) is $\log E_{dot} = 38.4$, which is one of the largest values among known PWNe. We can confirm it when we can detect the torus of the PWNe. The size estimated to be 0.39 pc, or 1.6 arcsec using the distance to the LMC of 50 kpc (Feast 1999), which can be detectable with excellent spatial resolution of Chandra, but not with XMM-Newton (Bamba et al. 2006).

6. Summary

We have made a systematic study of PWN spin down luminosity and tori radii using *Chandra* data of 11 samples. It is discovered, for the first time, that $\log r$ and $\log \dot{E}$ have very strong positive correlation. The tori could be X-ray emission originating from the outside of the termination shocks as suggested by Kennel & Coroniti (1984). The fluctuation in the correlation is mainly produced

by variation of the external pressure and distance uncertainties. With this correlation, we can estimate the spin-down luminosity and distance to the PWN without information of coherent pulsations. This estimation has been applied to G0.9+0.1, G328.4+0.2, PSR 1846–0258, and DEM L241.

The authors thank the anonymous referee for his/her suggestions. The authors also thank T. Dotani and Y. Terada for their comments. AB is supported by JSPS Research Fellowship for Young Scientists. The work of KM is partially supported by the Grant-in-Aid for Young Scientists (B) of the MEXT (No. 18740108).

REFERENCES

- Bamba, A., Ueno, M., Nakajima, H., Mori, K., & Koyama, K. 2006, *A&A*, 450, 585
- Becker, R. H., & Helfand, D. J. 1984, *ApJ*, 283, 154
- Camilo, F., Ransom, S. M., Gaensler, B. M., & Lorimer, D. R. 2009, *ApJ*, 700, L34
- Caraveo, P. A., De Luca, A., Mignani, R. P., & Bignami, G. F. 2001, *ApJ*, 561, 930
- Case, G. L., & Bhattacharya, D. 1998, *ApJ*, 504, 761
- Chen, Y., Wang, Q. D., Gotthelf, E. V., Jiang, B., Chu, Y.-H., & Gruendl, R. 2006, *ApJ*, 651, 237
- Cordes, J. M., & Lazio, T. J. W. 2002, arXiv:astro-ph/0207156
- Duncan, R. C., & Thompson, C. 1992, *ApJ*, 392, L9
- Feast, M. 1999, *PASP*, 111, 775
- Ferrario, L., & Wickramasinghe, D. 2006, *MNRAS*, 367, 1323
- Gaensler, B. M., & Wallace, B. J. 2003, *ApJ*, 594, 326
- Gaensler, B. M., Pivovarov, M. J., & Garmire, G. P. 2001, *ApJ*, 556, L107
- Gavriil, F. P., Gonzalez, M. E., Gotthelf, E. V., Kaspi, V. M., Livingstone, M. A., & Woods, P. M. 2008, *Science*, 319, 1802

- Gelfand, J. D., Gaensler, B. M., Slane, P. O., Patnaude, D. J., Hughes, J. P., & Camilo, F. 2007, *ApJ*, 663, 468
- Helfand, D. J., Collins, B. F., & Gotthelf, E. V. 2003, *ApJ*, 582, 783
- Kargaltsev, O., & Pavlov, G. G. 2008, 40 Years of Pulsars: Millisecond Pulsars, Magnetars and More, 983, 171 (Astro-ph/0801.2602)
- Kennel, C. F., & Coroniti, F. V. 1984, *ApJ*, 283, 694
- Koo, B.-C., et al. 2008, *ApJ*, 673, L147
- Kothes, R., Uyaniker, B., & Pineault, S. 2001, *ApJ*, 560, 236
- Kumar, H. S., & Safi-Harb, S. 2008, *ApJ*, 678, L43
- LaMassa, S. M., Slane, P. O., & de Jager, O. C. 2008, *ApJ*, 689, L121
- Lazendic, J. S., Dewey, D., Schulz, N. S., & Canizares, C. R. 2006, *ApJ*, 651, 250
- Leahy, D. A., & Tian, W. W. 2008, *A&A*, 480, L25
- Ng, C.-Y., & Romani, R. W. 2004, *ApJ*, 601, 479
- Ng, C.-Y., & Romani, R. W. 2008a, *ApJ*, 673, 411
- Ng, C.-Y., Slane, P. O., Gaensler, B. M., & Hughes, J. P. 2008b, *ApJ*, 686, 508
- Possenti, A., Cerutti, R., Colpi, M., & Mereghetti, S. 2002, *A&A*, 387, 993
- Rea, N., et al. 2009, *ApJ*, 703, L41
- Rees, M. J., & Gunn, J. E. 1974, *MNRAS*, 167, 1
- Roberts, D. A., Goss, W. M., Kalberla, P. M. W., Herbstmeier, U., & Schwarz, U. J. 1993, *A&A*, 274, 427
- Romani, R. W., Ng, C.-Y., Dodson, R., & Briskin, W. 2005, *ApJ*, 631, 480
- Tian, W. W., & Leahy, D. A. 2008, *MNRAS*, 391, L54
- Trimble, V., & Woltjer, L. 1971, *ApJ*, 163, L97
- Vink, J., & Kuiper, L. 2006, *MNRAS*, 370, L14
- Vink, J., & Bamba, A. 2009, submitted to *ApJ*, arXiv:0909.3843
- Weisskopf, M. C., et al. 2000, *ApJ*, 536, L81
- Yamaguchi, H., et al. 2008, *PASJ*, 60, 141

TABLE 1
PARAMETERS OF TORI OF PWNE

	radius (r_{arcsec}) [arcsec]	distance [kpc]	radius (r) [pc]	$\log \dot{E}$ [ergs s $^{-1}$]	$\log \tau$ [years]	References
PSR J0537–6910 (N157B)	4.0±0.58	50	0.97±0.14	38.68	3.70	(1) (4)
Crab ^a	41.33±0.20	2	0.400±0.002	38.66	3.09	(2) (5)
PSR B0540–69	2.35±0.06	50	0.57±0.01	38.17	3.22	(1) (4)
PSR J1833–1034 (G21.5–0.9) ...	5.7±0.2	4.8	0.133±0.004	37.52	3.69	(1) (6)
PSR J0205+6449 (3C58) ^a	16.3±0.3	3.2	0.253±0.005	37.43	3.73	(1) (7)
PSR J2229+6114	9.3±0.4	0.8	0.036±0.001	37.35	4.02	(2) (8)
PSR J1124–5916	0.9±0.1	6	0.026±0.003	37.07	3.46	(1) (9)
SNR G54.1+0.3	4.6±0.1	8	0.178±0.004	37.06	3.46	(2) (10)
Vela	21.25±0.50	0.29	0.030±0.001	36.86	4.05	(2) (11)
PSR B1706–44	3.30±0.13	3	0.048±0.002	36.53	4.23	(3) (12)
PSR B1800–21	3.1±0.5	3.8	0.057±0.009	36.34	3.21	(1) (13)

NOTE.—(1) Ng & Romani (2008a); (2) Ng & Romani (2004); (3) Romani et al. (2005); (4) Feast (1999); (5) Trimble & Woltjer (1971); (6) Tian & Leahy (2008); (7) Roberts et al. (1993); (8) Kothes et al. (2001); (9) Gaensler & Wallace (2003); (10) Koo et al. (2008); (11) Caraveo et al. (2001); (12) Romani et al. (2005); (13) Cordes & Lazio (2002)

^aWe used parameters for outer torus.

TABLE 2
 σ_0 VS. THE EXPECTED CORRELATION FACTOR AND THE PROBABILITY OF THE REQUIRED CORRELATION FACTOR **with eq.(3)**

σ_0	$\sigma_0/2$	$\langle A \rangle$	$P(A > 0.82)$
0.4.....	0.2	0.90	0.93
0.56.....	0.28	0.82	0.56
0.6.....	0.3	0.80	0.49
0.8.....	0.4	0.71	0.23
1.0.....	0.5	0.62	0.12

TABLE 3
 σ_0 VS. THE EXPECTED CORRELATION FACTOR AND THE PROBABILITY OF THE REQUIRED CORRELATION FACTOR WITH EQ.(5)

σ_0	$\sigma_0/2$	$\langle A \rangle$	$P(A > 0.93)$
0.2.....	0.1	0.98	1.00
0.3.....	0.15	0.95	0.79
0.36.....	0.18	0.93	0.56
0.4.....	0.2	0.91	0.42
0.6.....	0.3	0.83	0.11
0.8.....	0.4	0.74	0.04

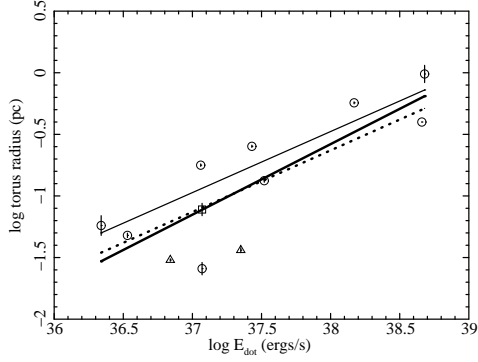


Fig. 1.— Spin-down luminosities vs. radii of tori. Triangles and circles are samples with/without interaction with interstellar medium or ejecta, while the box is a new estimation of the radius for PSR J1124–5916 (see text). Errors are quoted from Table 1. Thick solid and dashed lines represent eq.(3) and (4), whereas the thin solid line is for eq.(5).

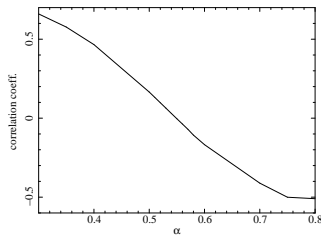


Fig. 2.— Correlation factors with different α .